First tomographic image of ionospheric outflows

E. Yizengaw,[1] M. B. Moldwin,[1] P. L. Dyson,[2] B. J. Fraser,[3] and S. Morley[3]

Received 28 July 2006; revised 8 September 2006; accepted 19 September 2006; published 19 October 2006.

[1] An image of the dayside low-energy ion outflow event that occurred on 16 December 2003 was constructed with ground- and space-based GPS (Global Positioning System) Total Electron Content (TEC) data and ion drift meter data from the DMSP (Defense Meteorological Satellite Program). A tomographic reconstruction technique has been applied to the GPS TEC data obtained from the GPS receiver on the Low Earth Orbit (LEO) satellite FedSat. The two dimensional tomographic image of the topside ionosphere and plasmasphere reveals a spectacular beam-like dayside ion outflow emanating from the cusp region. The transverse components of the magnetic field in FedSat's NewMag data show the presence of field aligned current (FAC) sheets, indicating the existence of low-energy electron precipitation in the cusp region. The DMSP ion drift data show upward ion drift velocities and upward fluxes of low-energy ions and electrons at the orbiting height of the DMSP spacecraft in the cusp region. This study presents the first tomographic image of the flux tube structure of ionospheric ion outflows from 0.13 Re up to 3.17 Re altitude.
Citation: Yizengaw, E., M. B. Moldwin, P. L. Dyson, B. J. Fraser, and S. Morley (2006), First tomographic image of ionospheric outflows, *Geophys. Res. Lett.*, *33*, L20102, doi:10.1029/2006GL027698.

1. Introduction

[2] The high-latitude ionosphere is an important source of the Earth's magnetospheric plasma [*Horwitz and Moore*, 1997; *Stevenson et al.*, 2000; *Strangeway et al.*, 2005; *Arvelius et al.*, 2005, and the references therein]. It is known that the dayside high-latitude cleft is one of the most important ionospheric outflow regions. Different techniques and instruments have observed large fluxes of upwelling ionospheric ions, particularly O^+. Earlier in situ observations presented some specific examples of well-defined outflows of O^+ [*Lockwood et al.*, 1985; *Stevenson et al.*, 2000; *Strangeway et al.*, 2005; *Arvelius et al.*, 2005]. However, none of these have shown the ion outflow as a function of altitude as their observations were restricted to the orbiting altitude of the particular satellite used. *Tu et al.* [2004], using IMAGE RPI (radio plasma imager), have extracted the density profiles in the polar cap along the field line using the active sounding technique. However, they did not specifically observe ion outflows.

[3] The dominant upwelling ion species below 3 R_E in the dayside cleft region is O^+ [*Pollock et al.*, 1990]. The question is what transports the ionospheric heavy ions (O^+) to higher altitude? Several mechanisms have been proposed to explain how ionospheric heavy ions gain additional momentum and escape to higher altitudes. Most of the earlier studies suggested that the potential mechanisms, which operate in the F-region and topside ionosphere, include: (1) upward thermal ion pressure caused by ion heating or ion production, which leads to thermal expansion of the plasma [e.g., *Wilson*, 1994]; (2) enhanced electron temperatures (via collisions with precipitating soft electrons, or other auroral thermal electron heating processes [e.g., *Wahlund et al.*, 1993]), which enhance ambipolar electric field acceleration [e.g., *Su et al.*, 1999]; (3) waves near the ion cyclotron or lower hybrid resonance frequencies, which drive perpendicular ion heating and subsequently parallel acceleration via the mirror force [e.g., *Ashour-Abdalla et al.*, 1981]. *Moore et al.* [1999] argued that fluctuations in the solar wind dynamic pressure itself drive the outflows. They suggested that such pressure fluctuations in turn drive Alfvén waves from the magnetopause into the high latitude ionosphere. These waves could then heat ions in the topside ionosphere, causing ion outflows. The enhanced Poynting flux flowing into the ionosphere could also heat the ions at high latitudes [*Strangeway et al.*, 2005], causing them to escape to higher altitude.

[4] This paper presents a tomographic image clearly showing an ion outflow event in the cusp region as a function of altitude. Tomographic imaging of topside ionospheric and plasmaspheric density using dual frequency band GPS receivers on LEO satellites gives us the ability to image the flux tube structure of ionospheric ion outflows, tracking the flux tube structure up to *3.17Re* (20,200 km) altitude for the first time. It shows a spectacular field-aligned tube-like density structure emanating from the cusp region of the ionosphere and escaping to higher altitude. This indicates that tomographic reconstruction techniques have the ability to detect narrow ionospheric ion outflows between the ionosphere and magnetosphere.

2. Data and Experiment Techniques

[5] LEO satellites that are equipped with dual-band frequency GPS receivers, such as FedSat [*Yizengaw et al.*, 2005], offer the opportunity for remote sensing and monitoring of the topside ionosphere and plasmasphere regions. GPS receivers on board continuously receive dual frequency signals transmitted by GPS satellites that broadcast two L-band signals at frequencies f_1 = 1.57542 *GHz* and f_2 = 1.2276 *Ghz*. Figure 1a shows the ground track of FedSat for the pass used in this study.

[1]Institute of Geophysics and Planetary Physics, University of California, Los Angeles, California, USA.
[2]Cooperative Research Center for Satellite System, Physics Department, La Trobe University, Bundoora, Victoria, Australia.
[3]Cooperative Research Center for Satellite Systems, Mathematical and Physical Sciences, University of Newcastle, Newcastle, New South Wales, Australia.

0094-8276/06/2006GL027698$05.00

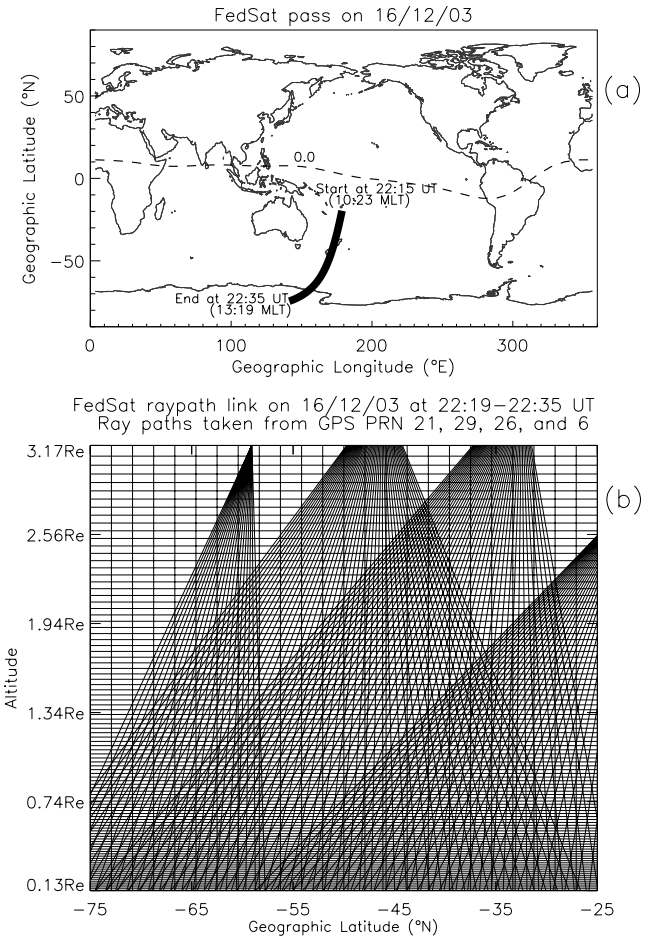

Figure 1. (a) Geographic map of FedSat ground track. The horizontal dashed line depicts the geomagnetic equator. (b) Tomographic imaging grid with an actual set of ray paths between LEO and GPS satellites for the FedSat satellite pass in Figure 1a. For clarity only one-third of the total ray paths are plotted.

[6] The integrated electron density along the ray path between the LEO GPS receiver and a GPS satellite, usually known as total electron content (TEC), can be derived from the combination of GPS pseudoranges ($P_1 - P_2$) and carrier phases ($L_1 - L_2$) [*Yizengaw et al.*, 2005]. However, by themselves, a series of TEC measurements are just a collection of line integrals of the free electron density and not maps of the electron density distribution or structure. In order to address the problem of imaging the electron density satisfactorily, a tomographic inversion method (based on a linear mathematical inversion) can be applied [*Yizengaw et al.*, 2005].

[7] Tomographic inversion methods essentially obtain maps of the free electron density from collections of GPS slant TEC observations across a region. The reconstruction plane is discretized into two-dimensional pixels [*Yizengaw and Moldwin*, 2005]. In space-based tomography the grid height spacing is not uniform, rather it increases as a function of altitude (see Figure 1b). By assuming that the electron density is constant in each pixel [*Tsai et al.*, 2002], the TEC along the ray path can then be represented as a finite sum of shorter integrals along segments of the ray path length [*Yizengaw et al.*, 2005]. The Global Plasmasphere Ionosphere Density (GPID) model [*Webb and Essex*, 2004] has been used to provide the initial guess for our Algebraic Reconstruction Tomography (ART) algorithm [*Yizengaw et al.*, 2005]. The technique of radio tomography has been widely used for the past two decades, and has been successfully verified using density profiles from incoherent scatter radar and ionosondes [e.g., *Pryse*, 2003; *Yizengaw et al.*, 2006, and the references therein].

3. Observation

[8] FedSat flew over New Zealand and the cusp region between 22:10 and 22:35 UT (09:10 – 09:35 LT) on 16 December 2003. Geomagnetic activity was weakly disturbed during that interval and the minimum *Dst* value was −28 *nT* at 18:00 UT. The *Kp* index was below 3 throughout the day. Auroral activity, however, was active with the AE index reaching approximately 1000 *nT* at 16:30 UT.

[9] The FedSat pass covered 5.0° S to 75.0° S geographic, transiting north-to-south at about 170° E longitude and between 22:10 UT and 22:35 UT. Figure 1b shows the ray path coverage, which is not uniform primarily because the GPS satellites move very little during the FedSat transit.

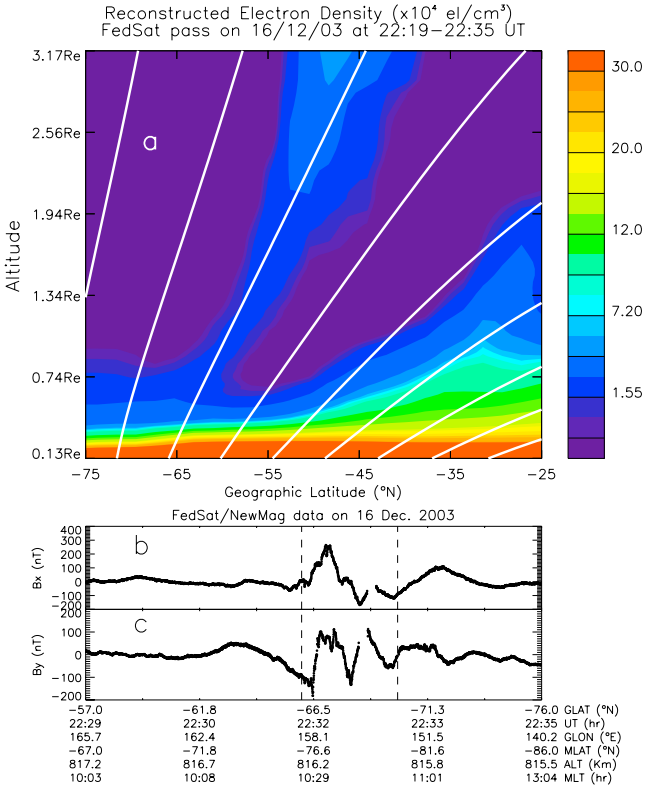

Figure 2. (a)Tomographically reconstructed density distribution using data recorded by GPS receiver on FedSat during the pass shown in Figure 1a. The curved white lines depict the magnetic field lines obtained from Tsyganenko 01-model. (b) The East-West transverse components of the FedSat NewMag magnetometer data (in a field-aligned frame) and (c) orthogonal component. The NewMag data has been rotated so that the Z direction corresponds to the IGRF total field vector.

Note, the ray paths shown here are taken only from the GPS satellites which were in ±15° longitude of FedSat's orbit longitude. Since the TEC gradient within ~30° longitude is insignificant, we merged these ray paths into a two-dimensional plane as shown in Figure 1b. In the analysis, pixels that are not crossed by LEO-GPS ray paths retain the density from the model initial guess as shown in the tomographic image output in Figure 2a. This figure shows the tomographically reconstructed electron density distribution in a two-dimensional (altitude versus geographic latitude) space region derived for this pass. The altitude range shown extends from 800 km (0.13Re) to 20200 km (3.2Re). Note, due to limited (approximately vertical) ray paths above 2.5 Re the density above this region may not be well constrained and the density above this height depends on the background density model. The white lines depict magnetic field lines generated using the Tsyganenko-01 model [*Tsyganenko*, 2002]. The color codes at the right indicate electron density ($\times 10^4$ el cm $^{-3}$). Note, a beam-like field aligned plume of enhanced density, extending from the topside ionosphere all the way up to the top of the image grid, is detected using the tomographic technique. The width of the density feature increases as a function of altitude. The density within the flux tube increases at higher altitude and reached up to 4.5 $\times$ 10^4 el cm $^{-3}$ from 3.5 $\times$ 10^4 el cm $^{-3}$at lower altitude. Otherwise, the figure shows a normal density distribution with higher density at lower latitudes than at high latitudes.

[10] Figures 2b and 2c show the transverse components of the FedSat NewMag magnetometer data in a field-aligned frame. The NewMag fluxgate magnetometer operates over 0-10Hz and is ideal for observing field aligned currents (FAC) [*Fraser*, 2003]. Figure 2c shows the East-West component of the magnetometer data and its orthogonal component is shown in Figure 2b. The NewMag data shows large perturbations in both transverse components, with the peak perturbations at about 68° S geographic latitude. This shows the presence of field-aligned current sheets, indicating the existence of low-energy electron precipitation [e.g., *Fraser*, 2003] in the cusp region where the ion outflows occurred. The field-aligned currents inferred from the magnetic perturbations are predominantly in the transverse components. The orientation of the FAC filament with respect to the FedSat trajectory determines which component shows the greatest perturbation. Generally, for Birkeland currents extended East-West (and with FedSat traveling predominantly North-South) the FAC should appear primarily in the Y component (Figure 2c) of NewMag data in the given reference frame.

[11] Several DMSP satellites circle the Earth in Sun-synchronous dawn-dusk orbits at about 900 km altitude. Figure 3 shows these quantities for the period when DMSP 15 was in its closest conjunction (in both time and space) with FedSat. The time difference is about 55 minutes with DMSP 15 transiting earlier than FedSat. The area between the two dashed lines in Figures 3b–3h indicates the region where the field aligned ion outflow was observed in the tomographic image. The DMSP vertical ion drift velocity is downward at equatorial and tropical latitudes and approximately zero at mid-latitudes before turning upward in the cusp region as shown in Figure 3b. The DMSP ion density (Figure 3c) also shows a significant density increase, i.e.,

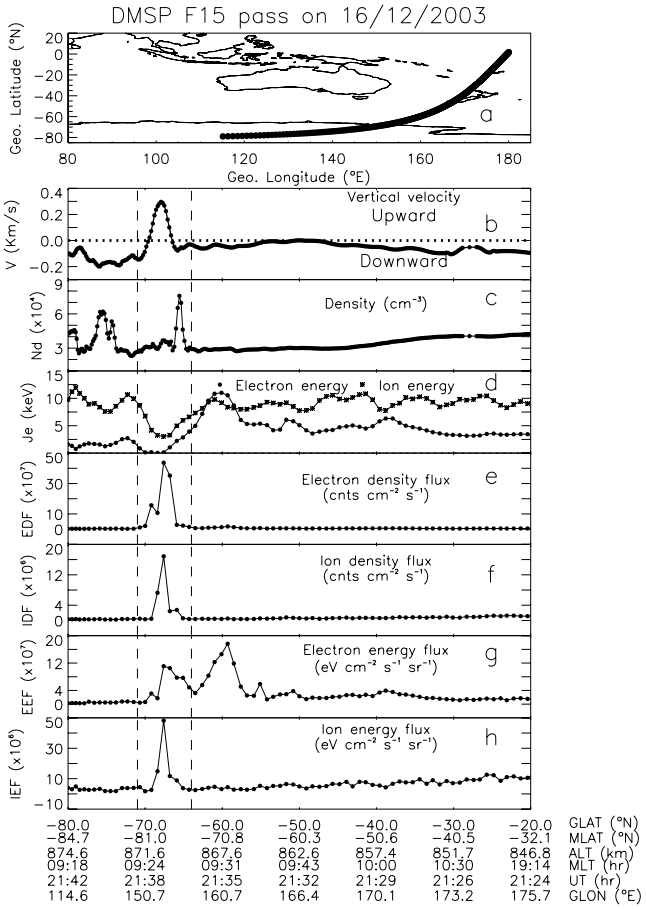

Figure 3. (a) DMSP F15 satellite pass on 16 December 2003. DMSP plasma data: (b) vertical velocity, (c) ion density, (d) ion and electron energy (e) electron density flux, (f) ion density flux, (g) electron energy flux, and (h) ion energy flux. The two dashed vertical lines indicate the region where the tomographic image observed a field aligned ion outflows.

from 2.5 $\times$ 10^4 el cm $^{-3}$ at equatorial and mid-latitudes to up to 8.0 $\times$ 10^4 el cm $^{-3}$ at the cusp region, which is about a 220% increase. The average energy of precipitating ions (stars) and electrons (dots), defined in each case as E_{AVE} = *E−Flux/N−Flux*, at the height of DMSP is also shown in Figure 3d. This indicates that electron and ion fluxes in the ionospheric ion outflow flux tube are low energy. Figures 3e–3h show electron and ion density and energy fluxes, respectively. They both show upward fluxes in the cusp region, indicating a peak value at about 67° S geographic or ~75° S geomagnetic latitudes. The upward electron energy flux, however, shows an extension equatorward, and a clear upward flux is evident at ~60.0° S geographic or 70.0° S geomagnetic latitude.

4. Discussion

[12] Previous studies have reported low-energy ionospheric ion outflows [*Arvelius et al.*, 2005]. Observations using data from CIS/CODIF instrument on Cluster spacecraft have clearly shown that the low-energy ion outflows are the dominant ionospheric outflows during magnetically

quiet periods ($Kp < 3$) [*Arvelius et al.*, 2005]. This is consistent with what we observed on 16 December 2003. We observed ionospheric outflows during a magnetically quiet period ($Kp< 3$) as shown in Figures 2 and 3. As can be seen in Figure 3d the DMSP ion drift meter data shows that the energy of ions and electrons was below 5 keV when the upward ion flows occur at the cusp region. The electron energy was at a lower level, just above 150 eV. The coordinated data from DMSP ion drift data and European Incoherent Scatter (EISCAT) Svalbard radar (ESR), reported by *Ogawa et al.* [2003], have shown that the average energy of electron precipitation in the cusp ion outflow region is below ~200 eV. *Ogawa et al.* [2003] have also shown that the peak energy of ions in the region is between 300 eV and 3 keV, with a low-energy cutoff occurring at 1–3 keV and below. These energy levels are consistent with the observation results shown in Figure 3d. Low-energy heavy ion flows should primarily exist in the lower ionosphere. This implies that there must be some process to bring them to higher altitude or even to the magnetosphere. The question is; what is the possible energizing mechanism that could provide momentum to the ionospheric heavy ions so they can escape to higher altitudes?

[13] The main possible heating mechanisms for low-energy ion outflows are wave-induced transverse heating [*Arvelius et al.*, 2005] or parallel acceleration due to field-aligned potential drops [*Norqvist et al.*, 1998]. At low altitude most O^+ heating and outflows are caused by ion energization associated with broad-band low frequency (BBLF) waves [*Norqvist et al.*, 1998]. Such a major source of O^+ ion energization is mostly located in the pre-noon time sector between 50° and 75° magnetic latitudes and at about 1400–1750 km altitude. The low energy of precipitating electrons in the cusp region also provides one of the mechanisms for heating heavy ions. The transverse components in the NewMag data (see Figures 2b and 2c) show the presence of FAC sheets, indicating the existence of low-energy electron precipitation in the cusp region where the ion outflows occurred. This heating mechanism could trigger the field-aligned ion outflows [*Strangeway et al.*, 2005; *Arvelius et al.*, 2005] shown in Figure 2a.

[14] Resonant wave heating, which mostly occurs below 2000 km altitude, may increase the perpendicular energy of ions, and the magnetic mirror force subsequently folds the ion distribution to become more beam-like at high altitudes [*Norqvist et al.*, 1998]. This is the type of structure clearly detected in the tomographic reconstruction image in Figure 2a between the altitudes of 5000 and 8000 km (078 Re – 1.25 Re), where the plasma structure is more field aligned, causing the density reduction at lower altitudes which is consistent with earlier observation by *Kintner et al.* [1996]. The cross sectional area of this field aligned ionospheric outflow appears to be wider at higher altitudes (>12000 km or 1.88 Re). This could be due to at least two reasons. The first one is due to the weakening of the magnetic field at high altitudes. Therefore, the flux tube area increases to keep the field aligned flux constant (i.e., $\oint B.d\mathrm{A}$=constant). The second possible reason may be due to additional heating mechanisms at higher altitudes that provide additional momentum or acceleration to the outflowing ionospheric ions. This could lead to particle diffusion, increasing the cross-section of the field aligned flux tube. Both Geotail and FAST spacecraft observations suggested that the cold outflowing O^+ ions are further energized up to ~2.7 keV at high altitude [*Seki et al.*, 2002]. A similar result has been reported that the cross sectional area of the flux tube of the accelerated ion outflows at high altitudes expanded toward the pole [*Arvelius et al.*, 2005].

[15] Plasma particle data from the DMSP satellite, shown in Figure 3, presents information about the plasma density and the ions and electron fluxes. The DMSP particle data are also used as confirmation of the tomographically observed field-aligned ion outflows shown in Figure 2a. The DMSP vertical drift shows upward flow at the cusp region as shown in Figure 3b. At the same time the ion density (see Figure 3c) indicates a density increase from $\sim 2.5 \times 10^4$ el cm^{-3} at equatorial and mid-latitudes to up to 8.0×10^4 el cm^{-3} in the cusp region, which is consistent with a similar observation reported by *Coley et al.* [2003]. The comparison between inferred density in Figure 2a and DMSP density in Figure 3c at about 0.12 Re shows that the inferred density is higher than DMSP density, and this could be due to the GPS receiver bias estimation error and the altitude averaging required for tomography. However, this does not affect the ability to observe TEC gradients, as it doesn't require absolute density to observe the ion outflow structure. A similar density enhancement in the cusp region is also observed by ground based GPS receivers located in the same region. Comparisons with the GPS TEC from nearby ground stations (not shown here) show that the GPS TEC in the cusp region has a slight increase, with a TEC peak centered at ~21:30 UT. However, the GPS TEC from GPS stations outside the cusp region did not show a similar enhancement. This indicates that the density enhancements are confined to the cusp region. According to current understanding one of the reasons for GPS TEC enhancements at high latitudes is the uplifting of plasma to higher altitudes where the recombination rate is low [*Yizengaw et al.*, 2005]. Therefore, the TEC enhancement in the cusp region could be due to the field-aligned ion outflow extending to higher altitudes, which is consistent with the observed ion outflows discussed above.

5. Conclusion

[16] Although there is about a 55 minute time gap between the tomographic observations (Figure 2a) and the DMSP plasma particle observation (Figure 3), both observations are consistent with narrowly confined (in latitude) ion outflows in the cusp region. Both ion and electron fluxes show striking upward flow as shown in Figures 3e–3h.

[17] Both ground- and space-based observations indicate that dayside ionospheric outflows were generally well confined to the cusp region. Most of the previous studies observed ion outflow at specific altitudes. This is the first observation showing the structure of the outflow as a function of altitude. These ion outflows were associated with heating due to low-energy precipitating electrons. The two-dimensional tomographic reconstruction approach to the space-based GPS TEC can reveal a more complete picture of field-aligned ion outflow emanating from the cusp region, indicating its ability to detect narrow ionospheric ion outflows between the ionosphere and magnetosphere. One of the main advantages of tomographic images is that they

can show the plasma transport between the ionosphere and magnetosphere, important information in understanding plasma flows such as the upward ion flow presented in this paper. Understanding plasma transport is essential to developing better models of ionospheric and plasmaspheric density, which are very important parameters for determining the space weather impact on precise positioning and communication systems.

[18] **Acknowledgments.** This research was supported in part by a NASA Guest Investigator grant (NNGO4GG343G), NSF grants (GEM/CEDAR post-doc fellowship (ATM-0524711) and ATM-0348398), and a JPL/UCLA partnership grant. Thanks are due to the IGS for the GPS data and NOAA Satellite and information service for DMSP ion drift data. The research was carried out with financial support from the Commonwealth of Australia through the Cooperative Research Centers (CRC) Program, and FedSat GPS data has been provided by the CRC for Satellite Systems. The magnetometer data was provided by the NewMag Magnetometer Team at the University of Newcastle.

References

Arvelius, S., et al. (2005), Statistics of high-altitude and high-latitude O^+ ion outflows observed by Cluster/CIS, *Ann. Geophys.*, *23*, 1909–1916.

Ashour-Abdalla, M., H. Okuda, and C. Z. Cheng (1981), Acceleration of heavy ions on auroral field lines, *Geophys. Res. Lett.*, *8*, 795–798.

Coley, W. R., R. A. Heelis, and M. R. Hairston (2003), High-latitude plasma outflow as measured by the DMSP spacecraft, *J. Geophys. Res.*, *108*(A12), 1441, doi:10.1029/2003JA009890.

Fraser, B. J. (2003), The FedSat microsatellite mission, *Space Sci. Rev.*, *107*, 303–306.

Horwitz, J. L., and T. E. Moore (1997), Four contemporary issues concerning ionospheric plasma flow to the magnetosphere, *Space Sci. Rev.*, *80*, 49–76.

Kintner, P. M., et al. (1996), SCIFER: Transverse ion acceleration and plasma waves, *Geophys. Res. Lett.*, *23*, 1873–1876.

Lockwood, M., et al. (1985), The cleft ion fountain, *J. Geophys. Res.*, *90*, 9736–9748.

Moore, T. E., et al. (1999), Ionospheric mass ejection in response to a coronal mass ejection, *Geophys. Res. Lett.*, *26*, 2339–2342.

Norqvist, P., M. André, and M. Tryland (1998), A statistical study of ion energization mechanisms in the auroral region, *J. Geophys. Res.*, *103*, 23,459–23,474.

Ogawa, Y., et al. (2003), Simultaneous EISCAT Svalbard radar and DMSP observations of ion upflow in the dayside polar ionosphere, *J. Geophys. Res.*, *108*(A3), 1101, doi:10.1029/2002JA009590.

Pollock, C. J., et al. (1990), A survey of upwelling ion event characteristics, *J. Geophys. Res.*, *95*, 18,969–18,980.

Pryse, S. E. (2003), Radio tomography: A new experimental technique, *Surv. Geophys.*, *24*, 1–38.

Seki, K., R. C. Elphic, M. F. Thomsen, J. Bonnell, J. P. McFadden, E. J. Lund, M. Hirahara, T. Terasawa, and T. Mukai (2002), A new perspective on plasma supply mechanisms to the magnetotail from a statistical comparison of dayside mirroring O^+ at low altitudes with lobe-mantle beams, *J. Geophys. Res.*, *107*(A4), 1047, doi:10.1029/2001JA900122.

Stevenson, B. A., et al. (2000), Relationship of O^+ field-aligned flows and densities to convection speed in the polar cap at 5000 km altitude, *J. Atmos. Sol. Terr. Phys.*, *62*, 495–503.

Strangeway, R. J., et al. (2005), Factors controlling ionospheric outflows as observed at intermediate altitudes, *J. Geophys. Res.*, *110*, A03221, doi:10.1029/2004JA010829.

Su, Y.-J., et al. (1999), Systematic modelling of soft-electron precipitation effects on high-latitude F region and topside ionospheric upflows, *J. Geophys. Res.*, *104*, 153–164.

Tsai, L. C., et al. (2002), Tomographic imaging of the ionosphere using the GPS/MET and NNSS data, *J. Atmos. Sol. Terr. Phys.*, *64*, 2003–2011.

Tsyganenko, N. (2002), A model of the near magnetosphere with a dawn-dusk asymmetry: 2. Parameterization and fitting to observations, *J. Geophys. Res.*, *107*(A8), 1176, doi:10.1029/2001JA000220.

Tu, J.-N., et al. (2004), Simulation of polar cap field-aligned electron density profiles measured with the IMAGE radio plasma imager, *J. Geophys. Res.*, *109*, A07206, doi:10.1029/2003JA010310.

Wahlund, J.-E., et al. (1993), Electron energization in the topside aurora1 ionosphere: On the importance of ion-acoustic turbulence, *J. Amos. Terr. Phys.*, *55*, 623–645.

Webb, P. A., and E. A. Essex (2004), A dynamic global model of the plasmasphere, *J. Atmos. Sol. Terr. Phys.*, *66*, 1057–1073.

Wilson, G. R. (1994), Kinetic modeling of O (+) upflows resulting from E x B convection heating in the high-latitude F region ionosphere, *J. Geophys. Res.*, *99*, 17,453–17,466.

Yizengaw, E., and M. B. Moldwin (2005), The altitude extension of the mid-latitude trough and its correlation with plasmapause position, *Geophys. Res. Lett.*, *32*, L09105 doi:10.1029/2005GL022854.

Yizengaw, E., et al. (2005), The Southern Hemisphere ionosphere and plasmasphere response to the interplanetary shock event of 29–31 October 2003, *J. Geophys. Res.*, A09S30 doi:10.1029/2004JA010920.

Yizengaw, E., M. B. Moldwin, P. L. Dyson, and E. A. Essex (2006), Using tomography of GPS TEC to routinely determine ionospheric average electron density profiles, *J. Atmos. Sol. Terr. Phys*, in press.

P. L. Dyson, Cooperative Research Center for Satellite System, Physics Department, La Trobe University, Bundoora, Victoria, Australia. (p.dyson@latrobe.edu.au)

B. J. Fraser and S. Morley, Cooperative Research Center for Satellite Systems, Mathematical and Physical Sciences, University of Newcastle, Newcastle, New South Wales, Australia. (brian.fraser@newcastle.edu.au, steven.morley@ newcastle.edu.au)

M. B. Moldwin and E. Yizengaw, Institute of Geophysics and Planetary Physics, University of California, Los Angeles, CA 90095, USA. (mmoldwin@igpp.ucla.educ; ekassie@igpp.ucla.edu)